Cellulose acetate graft copolymers with nano-structured architectures: Synthesis and characterization

ARTICLE *in* EUROPEAN POLYMER JOURNAL · MAY 2010

Impact Factor: 3.01 · DOI: 10.1016/j.eurpolymj.2010.01.021

European Polymer Journal 46 (2010) 944–957

Contents lists available at ScienceDirect

European Polymer Journal

journal homepage: www.elsevier.com/locate/europolj

Macromolecular Nanotechnology

Cellulose acetate graft copolymers with nano-structured architectures: Synthesis and characterization

M. Billy [a], A. Ranzani Da Costa [a], P. Lochon [a], R. Clément [a], M. Dresch [b], S. Etienne [c], J.M. Hiver [c], L. David [d], A. Jonquières [a,*]

[a] Laboratoire de Chimie Physique Macromoléculaire, UMR CNRS-INPL 7568, Nancy Université, ENSIC, 1 rue Grandville, BP 20451, 54 001 Nancy Cedex, France
[b] ADEME, 20 Avenue du Grésillé, BP 90406, 49 004 Angers Cedex, France
[c] Laboratoire de Physique des Matériaux, UMR CNRS 7556, École Nationale Supérieure des Mines, Nancy Université, Parc de Saurupt 54 042, Nancy, France
[d] Laboratoire des Matériaux Polymères et des Biomatériaux, Université de Lyon, Université Lyon 1, UMR 5223 IMP, Bât. ISTIL, 15, bvd Latarjet 69 622 Villeurbanne Cedex, France

ARTICLE INFO

Article history:
Received 11 June 2009
Received in revised form 11 January 2010
Accepted 24 January 2010
Available online 4 February 2010

Keywords:
Controlled free radical polymerization
Atom transfer radical polymerization
Grafting
Copolymer morphology

ABSTRACT

Cellulose acetate is a very good film-forming polymer with major applications in cigarette filters, photographic films, cosmetics and pharmaceutics formulations and membrane separation processes. Nevertheless, its rigidity and relative hydrophobic character can be limiting drawbacks for some applications. In this work, new cellulose acetate materials with highly flexible and hydrophilic grafts were obtained with different hydrophilic/hydrophobic balances. Cellulose acetate was grafted with methyl diethylene glycol methacrylate (MDEGMA) from brominated macroinitiators by atom transfer radical polymerization (ATRP) in two steps. The first step consisted of introducing ATRP initiator groups on cellulose acetate by reacting hydroxyl side groups with 2-bromoisobutyryl bromide. A preliminary study was then carried out to determine the experimental conditions for the controlled ATRP of MDEGMA homopolymerization in a solvent (cyclopentanone) compatible with cellulose acetate grafting. In these conditions, the MDEGMA homopolymerization followed Hanns Fischer's kinetics model accounting for the radical persistent effect. The ATRP grafting was then investigated for two cellulose acetate macroinitiators differing in the number of their ATRP initiator groups. Two families of graft copolymers with nano-structured architectures were obtained. The first family corresponded to copolymers with a high number of short grafts. The copolymers of the second family had almost the same graft weight fractions but a small number of long grafts. The morphology of the graft copolymers was then investigated by synchrotron X-ray scattering. The most informative results showed that the phase segregation depended upon the number and length of the poly(MDEGMA) grafts. The copolymer with 44 wt.% of long grafts showed a segregated morphology of nano-domains with sharp interfaces and a radius of gyration of 11.5 nm (from Guinier's law). These cellulose acetate copolymers eventually led to strong films with potential applications in membrane separations.

1. Introduction

Cellulose acetate is a very good film-forming polymer with a great range of worldwide industrial applications. Major examples relate to membrane separation processes, photographic films, cigarette filters, cosmetics and pharmaceutics formulations [1,2]. Nevertheless, its high glass transition temperature, rigidity and relative hydrophobic character can be limiting drawbacks for some applications. In this work, a controlled radical polymerization technique (atom transfer radical polymerization) is used to obtain cellulose acetate materials with highly flexible hydrophilic grafts and different hydrophilic/hydrophobic balances.

* Corresponding author.
E-mail address: Anne.Jonquieres@ensic.inpl-nancy.fr (A. Jonquières).

0014-3057/$ - see front matter © 2010 Elsevier Ltd. All rights reserved.
doi:10.1016/j.eurpolymj.2010.01.021

Independently discovered by Matyjaszewski and Sawamoto in 1995 [3,4], atom transfer radical polymerization (ATRP) is currently the most widely used controlled radical polymerization technique with an average yearly number of publications of ca. 700 [5]. The principle for the ATRP control is based on a reversible end-capping of the growing chains by a halide atom. This reversible end-capping involves an oxido-reduction leading to the homolytic cleavage of the terminal C-halide bond and the oxidation of a metal catalyst which is most usually a copper salt dissolved in the polymerization medium with a ligand.

Within this context of very strong international research activity, the grafting of cellulose (i.e. the cellulose acetate precursor) by ATRP appears much more recent and was first reported by Carlmark and Malmström in 2002 [6]. Since this pioneering paper, less than ten more papers have addressed the grafting of cellulose by ATRP [7–15]. In the former works, the grafting took place in heterogeneous medium, owing to the insolubility of cellulose in most organic solvents. Very recently, ten papers dealing with the ATRP grafting of cellulose derivatives have been published in the literature (Table 1). This topic of interest thus truly appears as an emerging and challenging field. Amongst these papers, three only reported the ATRP grafting of cellulose acetate. In the latter papers, the ATRP grafting was initiated from brominated or chlorinated macroinitiators (CA-Br, CA-Cl and CA-*g*-PCL-Br). The grafted monomers were leading industrial monomers (styrene, methyl methacrylate (MMA) and butyl acrylate

Table 1
Experimental results formerly reported for the ATRP grafting of cellulosic derivatives.

Ref.	Macro- initiator	DS_X	T (°C)	Monomer	Maximum conversion	*PDI* (calibration)
[28]	CA-Br	0.43	80	MMA	5.1% in 8 h	1.45 (PS)
			70		4% in 8 h	1.37 (PS)
					5.4% in 8 h	1.45 (PS)
[31]	EC-Br	0.5	110	Styrene	20% in 21 h 30	1.28[c] (PS)
			70	MMA	29% in 48 h	1.34[c] (PS)
[32]	EC-Br	0.04	80	*t*-BA	60% in 5 h	1.56 (PS)
		0.25			45% in 2 h 30	2.0 (PS)
[29]	CA-Br	0.12	110	Styrene	9% in 10 h	1.93 (PS)
					14% in 12 h	1.95 (PS)
		0.52			7% in 12 h	1.74 (PS)
					13% in 9 h	1.89 (PS)
		0.52	60	BA	15% in 8 h 30	1.51 (nr)
		0.12	70		25% in 5 h	1.68 (nr)
	CA-Cl	0.10	90	MMA	18% in 1 h 30	2.04 (PMMA)
					21% in 2 h 30	1.95 (PMMA)
		0.41	75		7% in 18 h	1.52 (PMMA)
[33]	EC-Br	0.52	85	MMAzo	19% in 24 h	nr
[34]	EC-Br	0.5	110	Styrene	20% in 21 h 30	1.27[c] (PS)
		0.04			10% in 10 h 30	1.16[c] (PS)
[22]	CA-*g*-CL1-Br	0.5	110	Styrene	7% in 8 h 30	1.50[c] (PS)
	CA-*g*-CL2-Br				7% in 8 h**	2.20[c] (PS)
			70	MMA	6% in 7 h	2.25[c]
	CA-*g*-CL3-Br				5% in 15 h	(PMMA)
	CA-*g*-CL1-Br		60	BA	3% in 24 h	1.51[c]
			70		5% in 11 h	(PMMA)
					10% in 8 h	1.87[c] (nr)
	CA-*g*-CL2-Br				6% in 7 h	1.47[c] (nr)
						2.64[c] (nr)
						2.56[c] (nr)
[35]	CPrOH-Br	2.26	70	MMA	24.8% in 48 h	nr
			80		39% in 19 h	nr
					10% in 20 h**	nr
[36]	EC-Br	0.09	30	HEMA	9.5% in 16 h	1.75 (PS)
			40		13.3% in 12 h	1.15 (PS)
		0.04	40		8.3% in 10 h	1.18 (PS)
[37]	CPrOH-*g*-CL-Br	2.9	70	*t*-BA	5% in 5 h	nr
					32% in 14 h	nr
[38]	EC-Br	0.02	60	PEGMA	60% in 14 h	1.48 (PS)
		0.2			55% in 8 h	1.41 (PS)

Ref., reference; T, temperature; DS_X, substitution degree of the initiator fragment (bond C–X with X: halogen); **, non-reproducible; nr, not reported; [c], cut grafts.

Cellulosic derivatives: CA, cellulose acetate; EC, ethyl cellulose; CPrOH, hydroxypropyl cellulose; CA-*g*-CL1-Br, functionalized cellulose acetate grafted by poly(ε-caprolactone) by ring opening polymerization with $DP_n = 89$; CA-*g*-CL2-Br, idem with $DP_n = 50$; CA-*g*-CL3-Br, idem with $DP_n = 38$; CPrOH-*g*-CL-Br, functionalized hydroxypropyl cellulose grafted by poly(ε-caprolactone) by ring opening polymerization.

Monomers: MMA, methyl methacrylate; MMAzo, 6-(4-(4-methoxyphenylazo)phenoxy)hexylmethacrylate; HEMA, 2-hydroxyethyl methacrylate; BA, butyl acrylate; T-BA, *tert*-butyl acrylate; PEGMA, poly(ethylene glycol) methyl ether methacrylate.

(BA)). The best results obtained for the ATRP grafting of cellulose acetate were obtained for very low conversion ($X \leqslant 15\%$) and the polydispersity index *PDI* was usually reported for the graft copolymers with $PDI \leqslant 1.5$ for styrene and $PDI > 1.5$ for MMA and BA.

In this work, the monomer methyl diethylene glycol methacrylate (MDEGMA) was chosen to lead to highly flexible grafts (the glass transition temperature of the corresponding homopolymer is close to −35 °C) with a strong hydrophilic character. A bibliography study indicates that the ATRP of MDEGMA has been very rarely reported and that the conditions used in the former studies cannot be directly transposed to our system because cellulose acetate is not soluble in the reported solvents [16,17].

The first part of this paper thus reports a fundamental investigation of the MDEGMA homopolymerization by ATRP. This investigation was carried out in order to find the proper experimental conditions to ensure the ATRP control for this particular monomer in a solvent compatible with cellulose acetate grafting. The second part of the paper reports the ATRP grafting of cellulose acetate with MDEGMA from two macroinitiators differing in the number of their ATRP initiator groups. On the basis of a kinetics investigation which shows the specificity of ATRP grafting from such macroinitiators, two families of copolymers are then described with almost the same graft weight fractions but either short or long grafts. Aiming at providing important micro-structural information on the graft copolymers, the last part of the paper analyzes the results of a first physical characterization by synchrotron small angle and wide angle X-ray scattering.

2. Experimental

2.1. Solvents and materials

Prior to use, cellulose acetate (CA, Fluka, acetyl 40 wt.%, M_W = 52,000 g/mol) was dissolved in 2-butanone at the concentration of 0.1 g/mL and then precipitated in a large excess of absolute ethanol and dried for five days in vacuum at 60 °C. The purified cellulose acetate was then stored in a tightly closed flask in a desiccator over sodium hydroxide. ^{1}H NMR analysis of the purified cellulose acetate in pyridine-d_5 confirmed its acetyl content, corresponding to 2.47 acetyl groups, and thus to 0.53 hydroxyl side groups, per glycosidic cycle. The degree of substitution for the acetyl groups, DS_{Ac}, is commonly defined as the number of acetyl groups per glycosidic ring and it is thus equal to 2.47 for this sample.

Ethyl 2-bromoisobutyrate (Aldrich, 98%) was used without further purification. 2-Bromoisobutyryl bromide (Alfa Aesar, 98%) was purified by fractioned vacuum distillation at 70 °C. Triethylamine (TEA, Aldrich, 99%) was distilled with sodium hydroxide under atmospheric pressure at 120 °C and stored under dry argon over 4 Å molecular sieves. Tetrahydrofuran (THF, VWR Prolabo) was distilled with sodium and benzoquinone under atmospheric pressure at 80 °C. This solvent was then kept in dark bottles under argon. Methyl diethylene glycol methacrylate (MDEGMA, Aldrich, 95%) was distilled under reduced pressure at 70 °C and stored at −20 °C under dry argon. Other reactants and solvents were used without purification.

2.2. Polymer synthesis

2.2.1. MDEGMA homopolymerization by ATRP

In a 25 mL Schlenk reactor, 2 g (11 mmol) of MDEGMA were stirred with 10 mL of cyclopentanone (Aldrich, 99%+). 45 microliters (0.2 mmol) of *N,N,N′,N″,N″*-pentamethyldiethylenetetramine (PMDETA, Aldrich, 99%) and 16 μL (0.1 mmol) of the initiator ethyl 2-bromoisobutyrate (Aldrich, 98%) were added with micro-syringes. The reaction mixture was degassed by three freeze–pump–thaw cycles. 10.5 mg (0.1 mmol) of CuCl (Acros, 99.99%) were then added under argon flow. The sealed reactor was immersed in an oil bath at the chosen temperature for the selected time. The reactor was then cooled down under water flow. The polymer was precipitated in 300 mL of petroleum ether. After careful washing, the petroleum ether was removed and the polymer was dried in vacuum for 2 h. The polymer was dissolved in chloroform and the solution was passed through alumina column for catalyst removal. If the solution was still turbid, it was filtrated through a PTFE micro-filter with 0.2 μm pores. Poly(MDEGMA) was eventually isolated as a rubbery solid by rotary evaporation.

The chemical shifts of the different protons of poly(MDEGMA) are presented thereafter for poly(MDEGMA) solutions in pyridine-d_5 at 300 MHz. ^{1}H NMR (300 MHz, pyridine-d_5) δ (ppm): 4,39 (s, 2H), 3,83 (s, 2H), 3,77 (s, 2H), 3,68 (s, 2H), 3,43 (s, 3H) 2,25 (m, 2H), 2,43 (m, 3H).

2.2.2. Macroinitiator synthesis

The synthesis of the macroinitiator with the lowest number of initiator groups (macroinitiator N°2) is presented as an example. The number of initiator groups can be increased by increasing the number of moles of 2-bromo isobutyryl bromide. Nevertheless, it appeared important to purify cellulose acetate prior to its chemical modification.

In a 500 mL three-necked round bottom flask, 29.3 g (110 mmol of glycosidic rings) of cellulose acetate were dissolved in 370 mL of anhydrous THF under argon flow and magnetic stirring. Then, 1.48 mL TEA (11 mmol) were added. 1.1 mL (8.8 mmol) of 2-bromo isobutyryl bromide with 5 mL of anhydrous THF were added dropwise. The mixture became slightly yellow–orange. The flask was filled with argon, sealed and left under stirring for 24 h at room temperature.

The macroinitiator was then precipitated in 2 L of absolute ethanol. It was dried and dissolved in 370 mL of 2-butanone and reprecipitated in 2 L of absolute ethanol for purification. The white product obtained at this stage was dried for five days in vacuum at 60 °C. Its composition was determined by bromine elementary analysis (bromine content: 0.33 wt.%). This bromine content corresponded to a degree of substitution for the initiator groups Z, DS_Z, equal to 0.01. Therefore, the macroinitiator obtained in this way contained 1 initiator group for 100 glycosidic rings.

2.2.3. MDEGMA grafting from macroinitiator N°1 (DS_Z = 0.06)

As a way of example, the procedure followed for the kinetics investigation in small batches is described

thereafter. In a 50 mL Schlenk reactor A, 0.2 g (0.7 mmol of glycosidic rings, corresponding to 0.04 mmol of initiating sites) of macroinitiator N°1 were dissolved in 16 mL of cyclopentanone. 0.8 g (4.2 mmol) of the monomer MDEGMA was then added. The reaction mixture A was degassed by three freeze–pump–thaw cycles and the reactor was filled with argon and sealed with a rubber septum.

In a 25 mL Schlenk reactor B, 4 mL of cyclopentanone and 19 μL (0.09 mmol) of PMDETA were mixed by magnetic stirring. This mixture was thoroughly degassed by bubbling argon gas. 4.39 mg (0.04 mmol) of CuCl was then added under argon flow and the reactor was sealed with a rubber septum.

The catalytic solution of reactor B was then transferred through a small stainless steel tube of 2 mm diameter into reactor A under argon flow. During this transfer, reactor A was connected to a cyclopentanone trap isolated from atmospheric humidity by a NaOH cartridge to prevent any overpressure in reactor A. After the transfer completion, reactor A was isolated and carefully stirred to obtain a homogeneous mixture. It was then immersed in an oil bath at 40 °C for the selected copolymerization time.

The reactor was then cooled down under water flow and the reaction mixture was passed through alumina column for catalyst removal. The column was carefully washed with acetone to obtain the maximal amount of copolymer. The mixture was then concentrated by rotary evaporation before the copolymer was precipitated in 150 mL of absolute ethanol before drying in vacuum at 60 °C for 8 h.

At this stage, the copolymer was obtained as a white solid which was then purified by dissolution in 10 mL of cyclopentanone and reprecipitation in 150 mL of absolute ethanol and eventually dried in vacuum at 60 °C overnight. Its composition was determined by ^{1}H NMR at 300 MHz (see main text).

2.2.4. MDEGMA grafting from macroinitiator N°2 (DS_Z = 0.01)

In a 25 mL Schlenk reactor, 0.5 g of macroinitiator N°2 (1.9 mmol of glycosidic rings, corresponding to 0.02 mmol of initiating sites) were dissolved in 10 mL of cyclopentanone. Thirty-two microliters (0.15 mmol) of PMDETA were added with a micro-syringe and 1.6 g (8.5 mmol) of the monomer MDEGMA in 2 mL of cyclopentanone were added. The reaction mixture was degassed by three freeze–pump–thaw cycles and 7.4 mg (0.075 mmol) of CuCl were then added under argon flow. The reactor was sealed under argon atmosphere and immersed in an oil bath at 40 °C under magnetic stirring.

After the selected copolymerization time, the reactor was cooled down under water flow and the copolymer was precipitated in 300 mL of absolute ethanol. After vacuum drying at 60 °C for 8 h, the copolymer was purified by dissolution in 8 mL of cyclopentanone and reprecipitation in 300 mL of absolute ethanol. After vacuum drying at 60 °C overnight, the copolymer was obtained as a white solid. Its composition was determined by ^{1}H NMR at 300 MHz (see main text).

2.2.5. Graft "cutting" by saponification in heterogeneous medium

In a 50 mL Erlenmeyer flask, 500.5 mg (1.1 mmol of glycosidic rings) of copolymer with DS_Z = 0.01 and 37% (w/w) of poly(MDEGMA) grafted chains were mixed with 25 mL of methanol and 205 mg (5.1 mmol) of NaOH. The saponification took place in heterogeneous medium at room temperature for 24 h. The final heterogeneous mixture was then filtered and the white solid residue was dried in vacuum at 60 °C. This solid residue was insoluble in common organic solvents and corresponded to cellulose. The filtrate, containing the poly(MDEGMA) grafts with sodium carboxylate end groups, was neutralized with HCl and NaCl was obtained as a side-product. After methanol evaporation, the poly(MDEGMA) grafts were recovered by extraction of the residual product with 25 mL of chloroform. After filtration and chloroform evaporation, the poly(MDEGMA) grafts were obtained as a slightly yellowish rubbery polymer which was characterized by ^{1}H NMR and size exclusion chromatography.

2.3. Polymer characterization

^{1}H and ^{13}C NMR spectra were recorded on a Bruker Avance 300 spectrometer at 300.15 MHz and 75.5 MHz, respectively. The chemical shifts were referenced to TMS and were calculated by using the residual isotopic impurities of the deuterated solvent. Elementary analyses were made by the Service Central d'Analyse of the Centre National de la Recherche Scientifique (USR 59 CNRS, Vernaison, France). The residual copper content was determined by the Service d'Analyse des Roches et Minéraux (SARM, Nancy, France).

For most of the samples, the average molar weights were determined by size exclusion chromatography (SEC) with a relative calibration using poly(ethyl methacrylate) standards for molecular weights in the range from 1650 g/mol to 139,000 g/mol. The corresponding Waters equipment used HPLC grade *N*,*N*-dimethylformamide solvent at a flow rate of 1 mL/min, a Styragel column and a Waters 410 differential refractometer. Ten milligrams of polymer were dissolved in 1 mL of *N*,*N*-dimethylformamide and filtered through PTFE micro-filters (Alltech, average pore diameter: 0.2 μm) prior injection. For a few samples, absolute molecular weight determination was also carried out with another Waters SEC equipment using two detectors. In addition to a Waters 410 differential refractometer, the second detector was a Multi-Angle Laser Light Scattering (MALLS) miniDAWN from Wyatt Technology. The calculation of *dn/dc* was performed using a calibration obtained from the differential refractometer. A value of *dn/dc* of 0.087 was found for poly(MDEGMA) homopolymers in *N*,*N*-dimethylformamide. The SEC–MALLS chromatograph was equipped with two PL gel 5 μm Mixed-D 300 × 7.5 mm columns in series and the polymer solutions were prepared as described formerly.

The short scale morphology of the graft copolymers was determined by means of X-ray scattering using polymer films with thicknesses of ca. 60 μm. Small angle and wide angle X-ray scattering (SAXS and WAXS, respectively) experiments were carried out at room temperature, without any additional thermal treatment, using synchrotron radiation at the European Synchrotron Radiation Facility (ESRF) in Grenoble. All the SAXS and WAXS experiments were performed on the BM2-D2AM beamline at an incident energy of 16 keV.

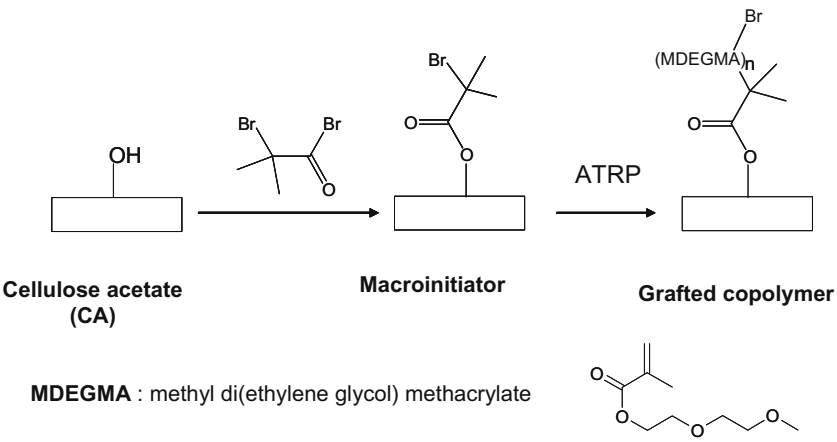

Fig. 1. Principle for the synthesis of the graft copolymers cellulose acetate-*g*-poly(MDEGMA) by atom transfer radical polymerization (ATRP).

3. Results and discussion

Cellulose acetate-*g*-poly(MDEGMA) copolymers were obtained by a "grafting from" method in two steps (Fig. 1). In a first step, cellulose acetate was functionalized to introduce C–bromine bonds acting as initiator groups for the ATRP. The number of the initiator groups introduced at this stage controlled the number of copolymer grafts. The second step consisted of polymerizing MDEGMA from the initiator groups in order to obtain the poly(MDEGMA) grafts with targeted lengths.

3.1. Homopolymerization of MDEGMA by ATRP

A preliminary investigation was first required to determine the proper conditions for the control of MDEGMA polymerization by ATRP. According to the literature, the ATRP of related methacrylic monomers was mainly carried out in strongly polar solvents at relatively high temperatures. Such solvents could not be used in this work because they do not dissolve cellulose acetate. It was particularly important that the solvent be compatible with cellulose acetate grafting in homogeneous medium and after a few preliminary experiments, cyclopentanone was eventually chosen for this investigation. The molecular initiator 2-bromoisobutyrate (EBriB) used in this work has the same type of chemical structure as the initiator groups later introduced on cellulose acetate. A mixed initiation system RBr/CuCl was chosen to take advantage of halide exchange to improve the ATRP control [18]. The ratio $[\text{initiator}]_0/[\text{CuCl}]_0$ was taken equal to 1. Amongst the ligands reported for ATRP, PMDETA is very widely used because it is commercially available and cheap. This ligand was chosen in this work with a typical ratio of $[\text{CuCl}]_0/[\text{PMDETA}]_0$ equal to ½.

Fig. 2 shows the results obtained at 60 °C and 40 °C in terms of number average molecular weight and polydispersity index *PDI*. At 60 °C, the molecular weights obtained with a relative SEC calibration with poly(ethyl methacrylate) standards varied linearly as a function of conversion despite some scattering of the data points (correlation coefficient $R^2 = 0.8513$). The polydispersity index remained less than 1.5 over the whole conversion range investigated in this work (0–80%). Decreasing the temperature by 20 °C improved the polymerization control as shown by the higher correlation coefficient ($R^2 = 0.9701$) for the linear variation of the molecular weights vs. conversion. Moreover, the corresponding polydispersity index remained less than 1.4 up to very high conversion (80%) for controlled radical polymerization. A molecular weight control was thus achieved at 40 °C.

Nevertheless and as expected, the experimental molecular weights with respect to poly(ethyl methacrylate) standards strongly differed from the theoretical ones (dashed line in Fig. 2) calculated from the monomer conversion *X* (determined by ^{1}H NMR of the polymerization medium) and the ratio of initial monomer concentration $[\text{MDEGMA}]_0$ over initial initiator concentration $[\text{EBriB}]_0$ by Eq. (1):

$$M_n^{th} = X \times \frac{[\text{MDEGMA}]_0}{[\text{EBriB}]_0} M_{\text{MDEGMA}} \quad (1)$$

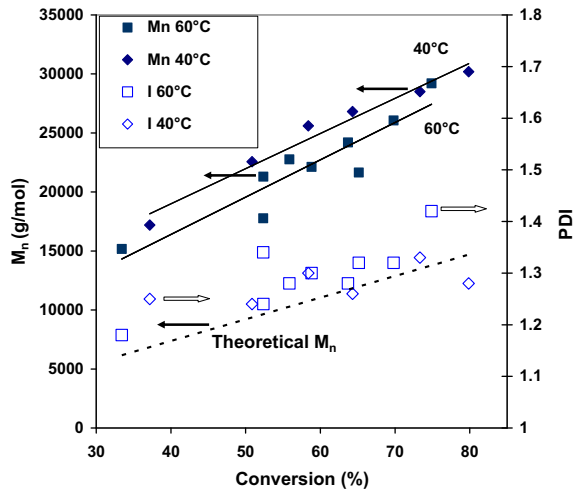

Fig. 2. Influence of temperature on homopolymerization of MDEGMA by ATRP. $[\text{MDEGMA}]_0 = 1.06$ mol/L, $[\text{EBriB}]_0 = 1.1 \times 10^{-2}$ mol/L, $[\text{EBriB}]_0/[\text{CuCl}]_0/[\text{PMDETA}]_0 = 1/1/2$. Results obtained by SEC analysis in *N*,*N*-dimethylformamide with poly(ethyl methacrylate) standards. Dashed line: theoretical M_n.

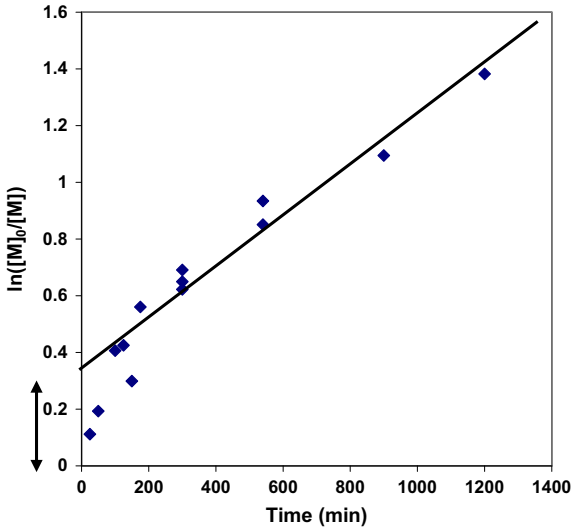

Fig. 3. Kinetics plot $\ln([M]_0/[M])$ vs. t for MDEGMA homopolymerization at 40 °C by ATRP. $[MDEGMA]_0 = 1.06$ mol/L, $[EBriB]_0 = 1.1 \times 10^{-2}$ mol/L, $[EBriB]_0/[CuCl]_0/[PMDETA]_0 = 1/1/2$. The double arrow points out the deviation from the linearity observed for the initial polymerization times.

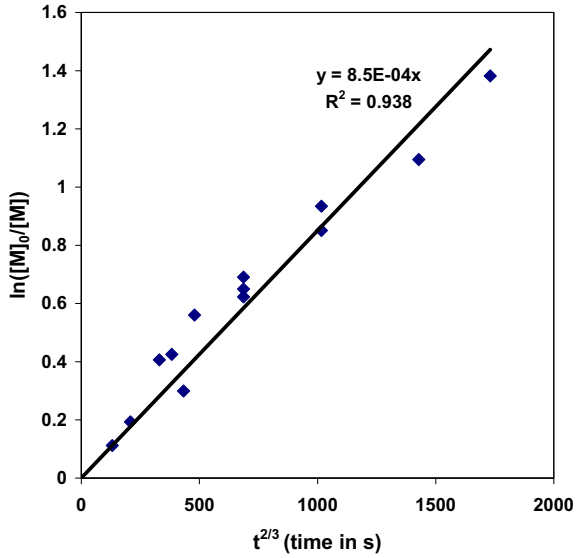

Fig. 4. Kinetics modelling of MDEGMA homopolymerization at 40 °C by ATRP according to Fischer's model: $\ln([M]_0/[M])$ vs. $t^{2/3}$. $[MDEGMA]_0 = 1.06$ mol/L, $[EBriB]_0 = 1.1 \times 10^{-2}$ mol/L, $[EBriB]_0/[CuCl]_0/[PMDETA]_0 = 1/1/2$.

Complementary SEC–MALLS experiments carried out with a few polymer samples led to absolute molecular weights and enabled to estimate the initiator efficiency. It was shown that the relative SEC calibration gave number average molecular weights overestimated by ca. 20% and that the initiator efficiency (given by the ratio of the theoretical molecular weights over the absolute molecular weights) was ca. 60% in these conditions.

The kinetics plot of $\ln([M]_0/[M])$ as a function of time at 40 °C (Fig. 3) was linear for polymerization times higher than 200 min but a significant deviation from linearity was observed for the initial polymerization times. Fig. 3 shows that the intercept of the linear plot corresponded to an initial value of almost 0.4. Therefore, the ATRP kinetics was not of first order with respect to monomer although we have shown that the main chain characteristics in terms of molecular weights and polydispersity index were well controlled. Such a deviant kinetics behavior was also observed by Hansen et al. for the ATRP of a closely related monomer (poly(oligo(ethylene glycol) methyl ether methacrylate PPEGMA) in organic medium [19]. Nevertheless, Fig. 4 shows that the ATRP kinetics data are in very good agreement with Fischer's model. This model [20] accounts for the persistent radical effect in controlled radical polymerization and forecasts a linear variation of $\ln([M]_0/[M])$ as a function of $t^{2/3}$, as it is typically observed in Fig. 4.

Consequently and although the kinetics behavior reflected the influence of the persistent radical effect, the ATRP homopolymerization of MDEGMA in cyclopentanone at 40 °C led to a good control over the molecular weights and polydispersity index for a very broad range of monomer conversion (0–80%).

3.2. Synthesis of cellulose acetate macroinitiators for ATRP

As a first step towards the grafting of cellulose acetate by ATRP, cellulose acetate macroinitiators with ATRP initiator groups were then obtained by a common procedure consisting of reacting hydroxyl side groups with 2-bromoisobutyryl bromide in anhydrous THF in presence of a base (triethylamine) capable of neutralizing the HCl side-product. Using a purified and carefully dried cellulose acetate was important to minimize the side reactions, in particular with residual water. By varying the amount of 2-bromoisobutyryl bromide, two macroinitiators were obtained with different numbers of initiator groups. ^{1}H NMR was not sensitive enough to characterize these macroinitiators and the very low degrees of substitution for the initiator groups, DS_Z, were thus determined by elementary analysis (bromine content).

Macroinitiator N°1 contained a high number of initiator groups (i.e. 6 initiatior groups for 100 glycosidic rings) and was the precursor of a first copolymer series with a high number of short grafts. In order to investigate the influence of macromolecular architecture on the properties of the graft copolymers, a second macroinitiator was then obtained with a small number of initiator groups (i.e. 1 initiatior group for 100 glycosidic rings). Macroinitiator 2 was the precursor for a second copolymer series with a small number of long grafts.

SEC experiments carried out with the CA precursor and both macroinitiators showed that there was no degradation of the CA backbone during its chemical modification at room temperature. Furthermore, the procedure of Tezuka and Tsuchiya [21] enabled to determine the regioselectivity of this chemical modification. This procedure characterizes the hydroxyl distribution on polysaccharides by quantitative ^{13}C NMR of their propionylated derivatives obtained by reacting the hydroxyl substituents with propionic anhydride quantitatively. Fig. 5a shows the NMR spectrum obtained for the propionylated cellulose acetate. According to Tezuka and Tsuchiya [21], the peaks in the

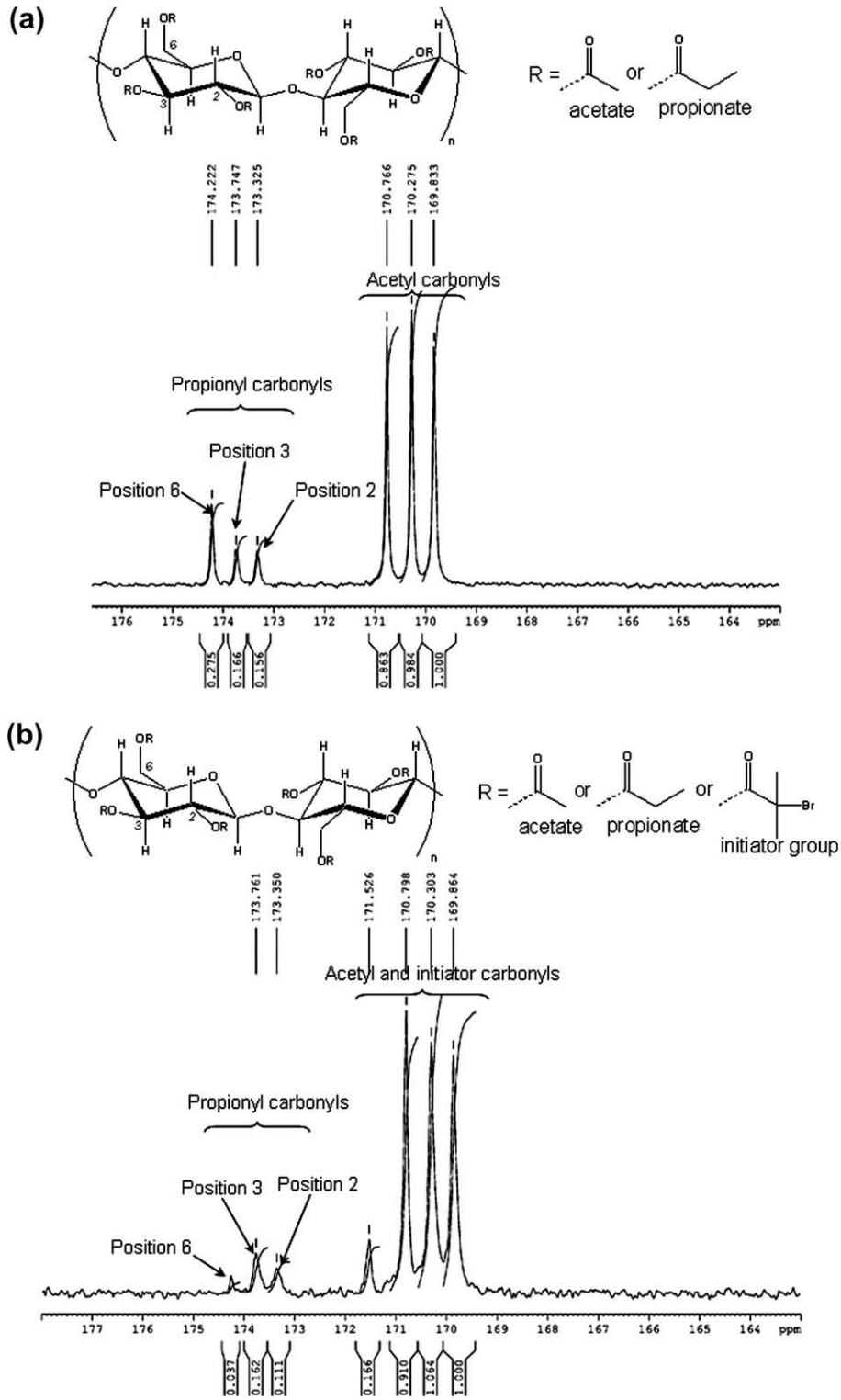

Fig. 5. Determination of the regioselectivity of the macroinitiator synthesis by ^{13}C NMR of the propionylated derivatives in $CDCl_3$ at 40 °C. Enlargement of the domain corresponding to the carbonyl groups: (a) for the cellulose acetate precursor, (b) for a macroinitiator with 25 initiator groups for 100 glycosidic rings.

range of 173–175 ppm are characteristic for the propionyl carbonyl groups and the positions 2, 3 and 6 correspond to the peaks with increasing chemical shifts. The total degree of substitution for the hydroxyl groups, DS_{OH}, can be easily

estimated from the ratio of the area corresponding to the propionyl carbonyls to the sum of the area corresponding to the acetyl and propionyl carbonyls:

$$DS_{OH} = \frac{A_{\text{propionyl}}}{A_{\text{propionyl}} + A_{\text{acteyl}}} = 0.53 \quad (2)$$

This result is in good agreement with that obtained by ^{1}H NMR and confirms that the reaction of the hydroxyl groups with propionic anhydride is quantitative. Therefore, the distribution of the hydroxyl substituents is the same as that of the propionyl carbonyls and can thus be estimated from Eq. (3) with $DS_{OH,p}$ standing for the degree of substitution for the hydroxyl groups in position p:

$$DS_{OH,p} = \frac{A_{\text{propionyl},p}}{A_{\text{propionyl}}} \times DS_{OH} \quad (3)$$

The following data were eventually obtained from the spectrum in Fig. 5a: $DS_{OH,2} = 0.13$, $DS_{OH,3} = 0.15$ and $DS_{OH,6} = 0.25$. These results are in good agreement with the much better reactivity of the position 6 during deacetylation of cellulose triacetate (i.e. the precursor for cellulose acetate). The same type of analysis was then carried out with a macroinitiator containing 25 initiator groups for 100 glycosidic rings (Fig. 5b). The choice of this macroinitiator was made to obtain a good sensitivity for the regioselectivity analysis. The results obtained from Fig. 5b are the following: $DS_{OH} = 0.27$, $DS_{OH,2} = 0.10$, $DS_{OH,3} = 0.14$ and $DS_{OH,6} = 0.03$. These data show that ca. 85%, 11% and 4% of the ATRP initiator groups are in positions 6, 2 and 3, respectively. As expected, the great majority of the ATRP initiator groups are thus in position 6 and the macroinitiator synthesis appears fairly regioselective.

3.3. Kinetics investigation of MDEGMA grafting from macroinitiator N°1 containing 6 initiator groups for 100 glycosidic rings

Our study globally aimed at obtaining relatively large amounts (ca. 5 g) of copolymers with increasing weight fractions of poly(MDEGMA) grafts in the range of 10–50 wt.%. In order to find the appropriate polymerization conditions, a first kinetics investigation was first carried out on a much smaller scale (300 mg) to spare both macroinitiator and monomer.

The simple transposition of the experimental conditions formerly determined for the MDEGMA homopolymerization quickly led to the partial gelification of the copolymerization medium. The particularly high reactivity of macroinitiator N°1 obviously led to some intermolecular recombination of the growing grafts. This problem was simply overcome by diluting the copolymerization medium by a factor 5 with cyclopentanone. The purification of the graft copolymers was then achieved by filtration over alumina column and double precipitation in ethanol which is both a solvent for the homopolymer poly(MDEGMA) and a non-solvent for the targeted graft copolymers.

The composition of the graft copolymers and the corresponding monomer conversion were then determined by

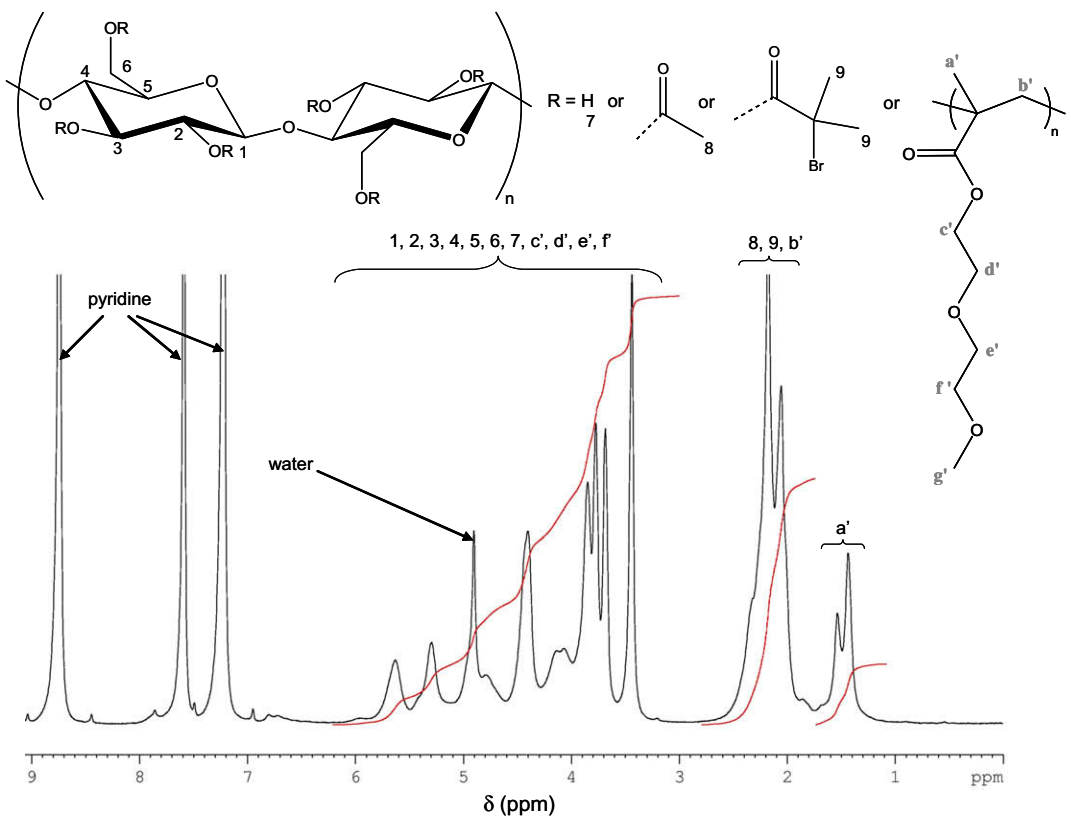

Fig. 6. ^{1}H NMR characterization of the graft copolymers (Pyridine-d_5, 300 MHz).

^{1}H NMR spectroscopy. Fig. 6 shows a typical spectrum obtained for a cellulose acetate-*g*-poly(MDEGMA) copolymer. This spectrum was recorded in pyridine-d_5 to shift the peak corresponding to residual water in a region which is not critical for the composition and conversion calculation. On the ^{1}H NMR spectrum, the signals related to the poly(MDEGMA) grafts clearly appeared in addition to those corresponding to the cellulose acetate macroinitiator. Despite its apparent complexity, the spectrum was characterized by three domains corresponding to the following integrated areas:

- A_1, the area for the peaks appearing between 1.7 and 2.6 ppm corresponded to the protons of the acetyl groups, the protons of the initiator groups *Z* and the two protons of the graft copolymer backbone, i.e. to $3 \times 2.47 + 6 \times DS_Z + 2 \times DS_Z \times DP_n$ protons, where DP_n is the number average polymerization degree for the poly(MDEGMA) grafts.
- A_2, the area for the peaks between 3 and 6 ppm corresponded to the seven protons of the glycosidic ring, the residual hydroxyl protons, the ethoxylenic protons c′ to f′ of the poly(MDEGMA) grafts and to the protons of the residual water in pyridine-d_5.
- A_3, the area for the peaks between 1.2 and 1.7 ppm corresponded to the methyl groups of the poly(MDEGMA) grafts and thus to $3 \times DS_Z \times DP_n$ protons.

The ratio of A_1 to A_3 was thus easily expressed as a function of the degree of substitution for the initiator groups *Z*, DS_Z, obtained from elementary analysis (here $DS_Z = 0.06$ for macroinitiator N°1) and the number average degree of polymerization DP_n of the poly(MDEGMA) grafts:

$$\frac{A_1}{A_3} = \frac{7.41 + 6 \times DS_Z + 2 \times DS_Z \times DP_n}{3 \times DS_Z \times DP_n} \quad (4)$$

A simple rearrangement of Eq. (4) thus gave the number average degree of polymerization DP_n of the poly(MDEGMA) grafts as a function of the ratio of A_1 to A_3 and the degree of substitution for the initiator groups *Z*, DS_Z:

$$DP_n = \frac{1}{DS_Z} \times \frac{7.41 + 6 \times DS_Z}{3 \times \frac{A_1}{A_3} - 2} \quad (5)$$

The corresponding monomer conversion *X* was then calculated from the number average degree of polymerization DP_n of the poly(MDEGMA) grafts by Eq. (6):

$$X = 1 - \frac{[M]}{[M]_0} = DP_n \times \frac{[\text{initiator}]_0}{[\text{MDEGMA}]_0} \quad (6)$$

Fig. 7 shows the corresponding results obtained for increasing copolymerization times. A first plot (Fig. 7a) of $\ln(\ln([M]_0/[M]))$ vs. time corresponded to a formal treatment of the kinetics data according to Fischer's model. It shows that the corresponding slope (1/2) seems to be less than the expected value of 2/3, even if some caution should be taken owing to some scattering of the experimental data (correlation coefficient $R^2 = 0.899$) quite typical for such type of grafting experiments. The second plot (Fig 7b) characterized the kinetics behavior by a linear dependency of $\ln([M]_0/[M])$ vs. $t^{1/2}$ with a correlation coefficient of $R^2 = 0.891$ for conversions up to 20%.

The characterization of the real molecular weight distribution of the poly(MDEGMA) grafts is quite complex and

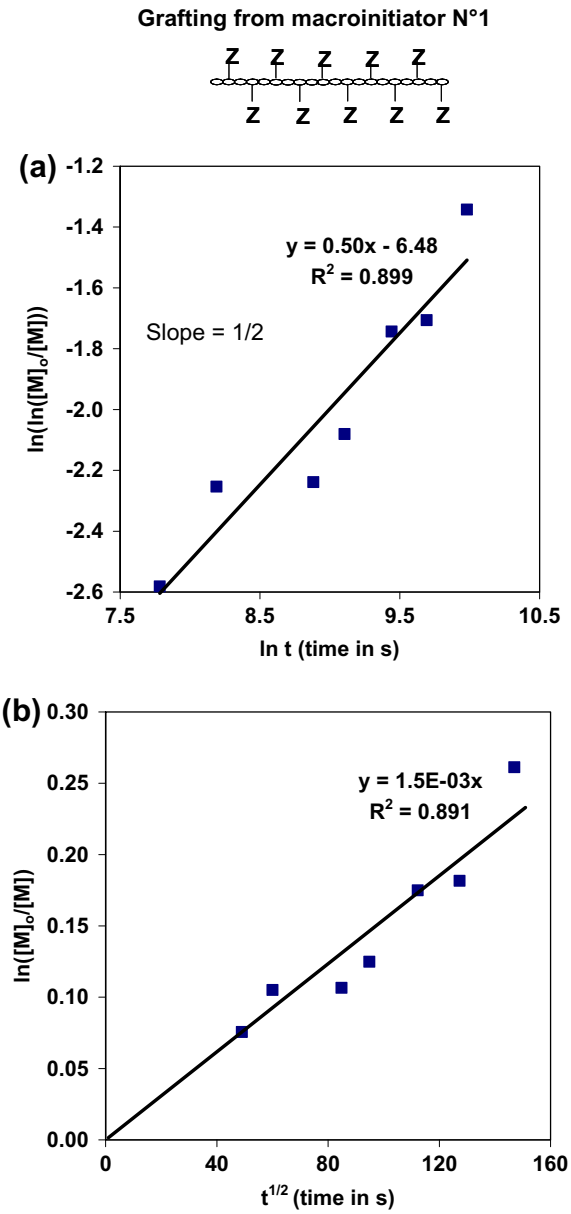

Fig. 7. Kinetics results obtained for cellulose acetate grafting by MDEGMA from macroinitiator N°1 leading to copolymers GS with a high number of short grafts. $[\text{MDEGMA}]_0 = 0.21$ mol/L, $[\text{initiator}]_0 = 2.2 \times 10^{-3}$ mol/L, $[\text{initiator}]_0/[\text{CuCl}]_0/[\text{PMDETA}]_0 = 1/1/2$.

could not be carried out on the small samples obtained during this kinetics investigation. Nevertheless, it will be reported later in this paper for some copolymer samples obtained on a larger scale.

3.4. Kinetics investigation of MDEGMA grafting from macroinitiator N°2 containing 1 initiator group for 100 glycosidic rings

Macroinitiator N°2 was then used to obtain a second copolymer series with a small number of long grafts. A preliminary study was carried out on small samples to

determine the kinetics behavior of the copolymerization with the new macroinitiator.

The first grafting attempts were performed in the same conditions as those for the controlled MDEGMA homopolymerization at 40 °C. However, in this case, the very low number of initiator groups imposed a high macroinitiator concentration to keep the concentration of initiator groups constant between both series of experiments. In these conditions, the macroinitiator was very poorly soluble and it had to be diluted by cyclopentanone to ensure its proper solubilization in the highly viscous copolymerization medium. Its concentration was eventually chosen to ensure the same concentration of the initiator groups as that used for the MDEGMA grafting from macroinitiator N°1. All the other parameters were kept identical to those defined for the controlled MDEGMA homopolymerization in order to obtain a reasonable copolymerization rate.

Fig. 8 shows the kinetics behavior obtained for the MDEGMA grafting from macroinitiator N°2. In the same way as for macroinitiator N°1, Fig. 8a shows a plot of $\ln(\ln([M]_0/[M]))$ vs. time. Once again, this plot is linear but its slope (0.39) is even lower than that obtained with macroinitiator N°1 with less scattering of the experimental data (correlation coefficient $R^2 = 0.94$). Accordingly, a second plot of $\ln([M]_0/[M])$ vs. $t^{0.39}$ is a straight line through origin which well accounts for the kinetics behavior over the whole investigated conversion range up to ca. 25% (correlation coefficient of $R^2 = 0.919$) (Fig. 8b).

Therefore, it appears that, even if the MDEGMA homopolymerization follows Fischer's model ($n = 2/3$), the MDEGMA grafting from both cellulosic macroinitiators deviates from this original model. Moreover, the characteristic kinetics parameter n decreases slightly (−20%) when the number of initiator groups present on the macroinitiator decreases. The corresponding copolymerization rate decrease could be related to an increase in viscosity observed for these highly viscous cellulosic systems and/or to a lower accessibility of the initiator groups when they are becoming less and less numerous on the macroinitiator.

3.5. Copolymer synthesis scaling-up

On the basis of the former kinetics data, the copolymer synthesis scaling-up then enabled to obtain two families of relatively large copolymer samples (ca. 5 g) with close graft weight fractions but different architectures (Table 2).

The scaling-up of the graft copolymer synthesis was carried out by simply transposing the experimental conditions used for the former kinetics investigation. The amounts of grafts in the copolymers were thus controlled by the copolymerization time.

The scaling-up with macroinitiator N°1 led to copolymers with 25, 40 and 48 wt.% of short grafts. Nevertheless, the lengths of the grafts obtained during this first scaling-up, with a macroinitiator containing a high number of initiator groups, were usually almost twice the lengths of the grafts which had been obtained during the corresponding kinetics investigation on a much smaller scale (cf. Section 3.3). Even after the drastic purification steps (column chromatography/double precipitation in ethanol), the residual copper content in the copolymers

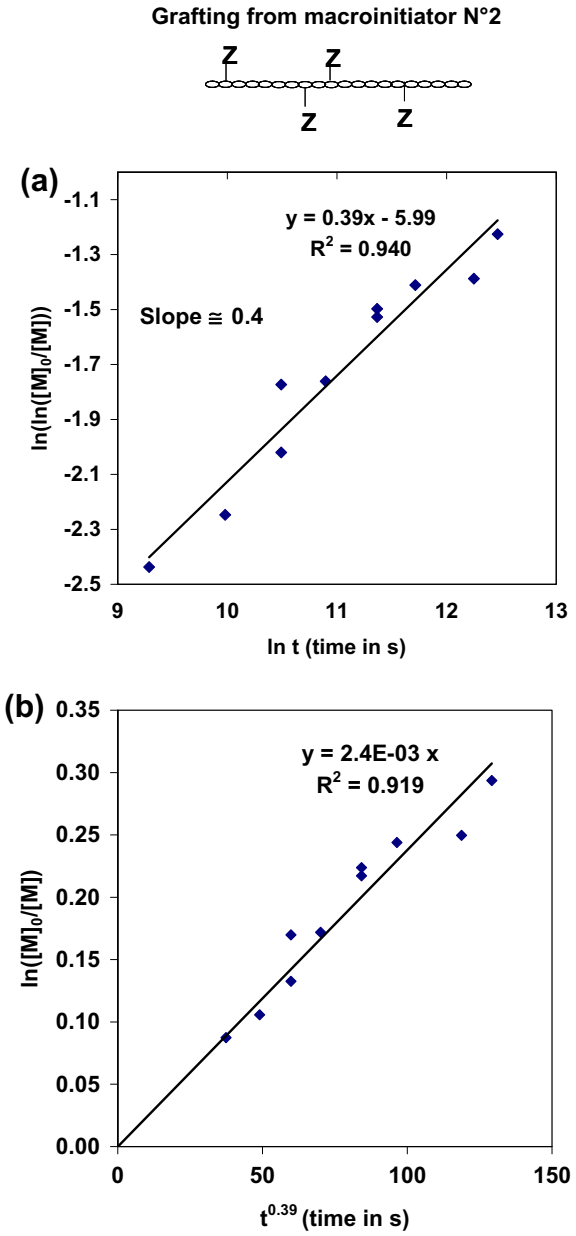

Fig. 8. Kinetics results obtained for cellulose acetate grafting by MDEGMA from macroinitiator N°2 leading to copolymers GL with a small number of long grafts. $[MDEGMA]_0 = 1.06$ mol/L, $[initiator]_0 = 2.1 \times 10^{-3}$ mol/L, $[initiator]_0/[CuCl]_0/[PMDETA]_0 = 0.21/1/2$.

was still ca. 100 ppm. The residual copper could be responsible for a further copolymerization occurring during the long solvent evaporation step at 50 °C. In good agreement with the former assumption, the scaling-up with macroinitiator N°2 – which contained much less initiator groups and thus required much less copper for ATRP – gave graft lengths which were much closer to those formerly obtained on a smaller scale with macroinitiator N°2. The success of the scaling-up with macroinitiator N°2 eventually led to graft copolymers with 25, 37 and 44 wt.% of long grafts (Table 2).

Table 2
Characteristics of the graft copolymers obtained after synthesis scaling-up leading to copolymer samples of ca. 5 g necessary for the physical and future permeability investigations.

Copolymer	ω_{grafts}	DP_n (g/mol) (^{1}H NMR)
Grafting from macroinitiator N°1 (6 initiator groups for 100 glycosidic rings)		
GS25	0.25	8
GS40	0.40	15
GS48	0.48	21
Grafting from macroinitiator N°2 (1 initiator group for 100 glycosidic rings)		
GL25	0.25	41
GL37	0.37	74
GL44	0.44	98

ω_{grafts}, graft weight fraction in the graft copolymers; DP_n (^{1}H NMR), number average degree of polymerization for the grafts determined by copolymer ^{1}H NMR analysis; GSX, copolymer with X% w/w of short grafts; GLX, copolymer with X% w/w of long grafts.

Table 3
Size exclusion chromatography (SEC) characterization of the poly(-MDEGMA) grafts. Analysis performed by SEC in *N*,*N*-dimethylformamide with poly(ethyl methacrylate) standards after saponification and neutralization of the graft copolymers in methanol.

Copolymer	Conversion (%)	M_n (g/mol)	*PDI*
Grafting from macroinitiator N°1 (6 initiator groups for 100 glycosidic rings)			
GS25	8	4790	≈1.49
GS40	16	5770	≈1.39
Grafting from macroinitiator N°2 (1 initiator group for 100 glycosidic rings)			
GL25	8	22,540	1.34
GL44	19	112,400	>1.5

GSX, copolymer with X% w/w of short grafts; GLX, copolymer with X% w/w of long grafts.
M_n, Number average molecular weight for the cut grafts; *PDI*, polydispersity index for the cut grafts.

The obtaining of relatively large amounts of copolymer samples then opened the way for characterizing the graft molecular weight distribution. The principle for this characterization first consisted of "cutting" the grafts and then analyzing their molecular weight distribution by size exclusion chromatography. Although rarely reported in the related literature, this characterization on the actual grafts is important for truly assessing the control of the ATRP grafting from cellulosic derivatives. Inspired by a procedure recently described by Vlcek et al. [22] for the analysis of polystyrene grafts for complex cellulosic copolymers, a method of copolymer saponification in methanol was then successfully developed in this work. Complementary (control) experiments carried out with cellulose acetate and the poly(MDEGMA) homopolymer showed that they were not degraded in the same conditions. Although the new method was rather complex and time-consuming, it enabled to obtain cut grafts in sufficient amount for molecular weight determination by size exclusion chromatography. Table 3 eventually summarizes the results obtained for the characterization of the poly-(MDEGMA) grafts for two copolymers per family.

The short grafts obtained from macroinitiator N°1 led to complex chromatograms with broad peaks for the lowest elution volumes, most likely owing to some aggregation induced by the numerous carboxylic end groups obtained after neutralization (Fig. 9). The number average molecular weights (M_n = 4790 and 5770 g/mol) reported in Table 3 were thus estimated from the thin peak corresponding to

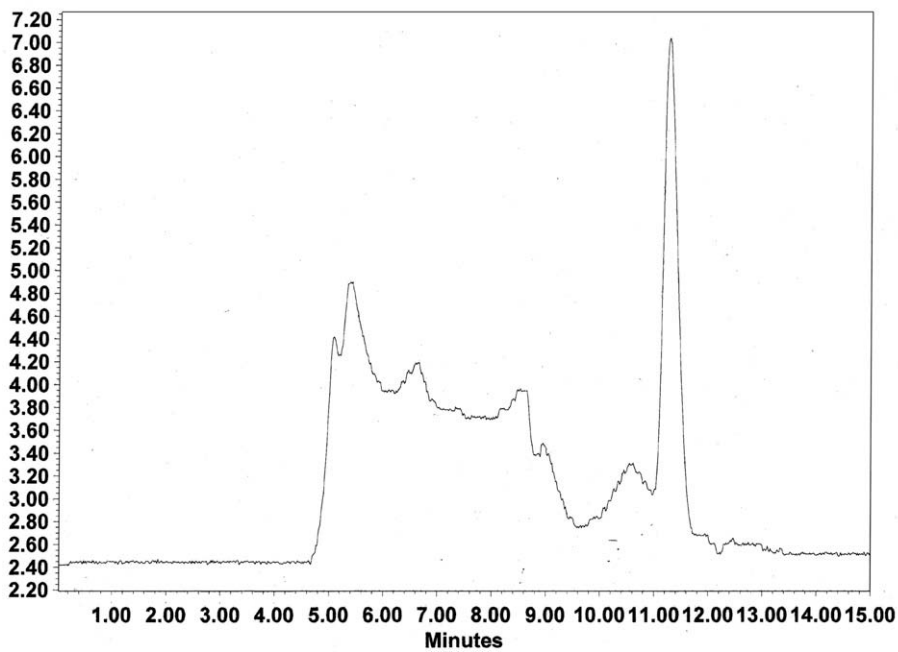

Fig. 9. Typical example for a SEC chromatogram obtained for the short grafts after the graft "cutting" from the cellulose acetate backbone.

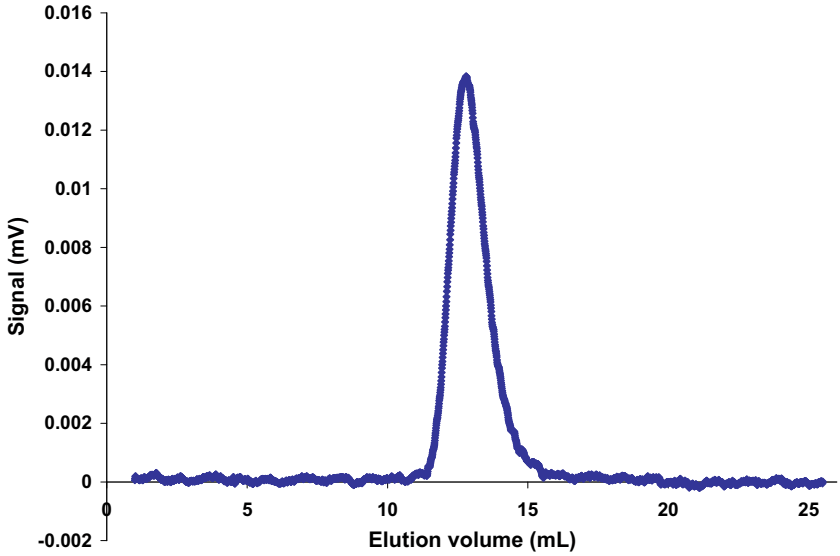

Fig. 10. Typical example for a SEC chromatogram obtained for the long grafts after the graft "cutting" from the cellulose acetate backbone. (SEC/MALLS experiment).

the highest elution volumes. Even if this simple calculation can be debated because it assumes that the aggregated grafts display the same characteristics as the individual grafts, it shows that the polymolecularity indexes were at best close to the limit value of 1.5 for controlled radical polymerization. As expected, the long grafts obtained from macroinitiator N°2 were much easier to characterize by size exclusion chromatography and the corresponding chromatograms showed a single thin peak (Fig. 10). No aggregation was thus detected for these long grafts with very few carboxylic end groups. The number average molecular weights obtained for the copolymers with 25 and 44 wt.% of long grafts were 22,540 and 112,400 g/mol, respectively. Nevertheless, in the latter case, the polydispersity index was higher than 1.5.

To conclude on this part, even if the control of ATRP was not truly achieved in these conditions, the grafting scaling-up enabled to vary the amount of the poly(MDEGMA) grafts within the range of interest. Two complementary series of copolymers with almost the same compositions and different architectures were eventually obtained.

3.6. Morphology characterization of the graft copolymers by WAXS and SAXS

As an illustration of the interest of the former synthesis routes for the elaboration of glycopolymers with tailor-made architectures, the morphology – which is believed to play a key role on their permeability properties – of the copolymers of both series was then investigated. The first experiments were carried out by differential scanning calorimetry (DSC). Unfortunately, DSC was not sensitive enough to detect the thermal transitions related to the grafts. Wide angle and small angle X-ray scattering experiments were then performed at the European Synchrotron Radiation Facility (ESRF – Grenoble) in order to assess the short scale morphology of the graft copolymers.

Fig. 11 shows the wide angle scattering pattern displaying the scattered intensity I as a function of the scattering vector $q = 4\pi(\sin\theta)/\lambda$ for cellulose acetate and the graft copolymers with long (GL) or short (GS) grafts. All the polymers displayed a halo with no clear Bragg peak which is characteristic for amorphous samples [23]. The diffraction pattern of cellulose acetate was slightly more complex with a major halo consisting in a first contribution observed at low q values close to 1.26 $Å^{-1}$ and another one at higher q at $q = 1.55$ $Å^{-1}$. These results are in agreement with previous published data for cellulose acetate with similar acetyl degree of substitution and produced in homogeneous conditions from bacterial cellulose [24]

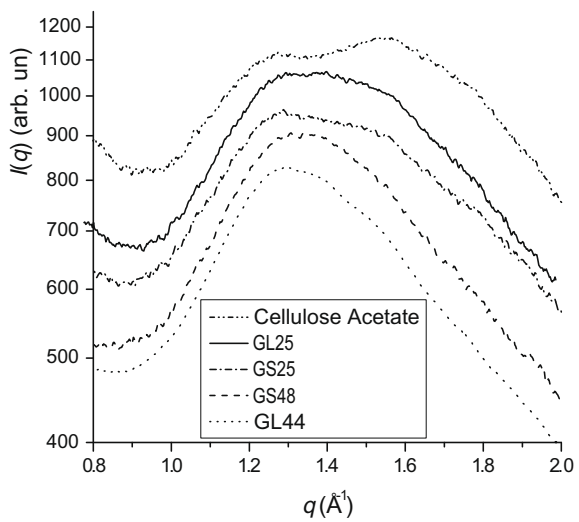

Fig. 11. Synchrotron wide angle X-ray scattering (WAXS) obtained for cellulose acetate and cellulose acetate-g-poly(MDEGMA) copolymers with long (GL) or short (GS) grafts.

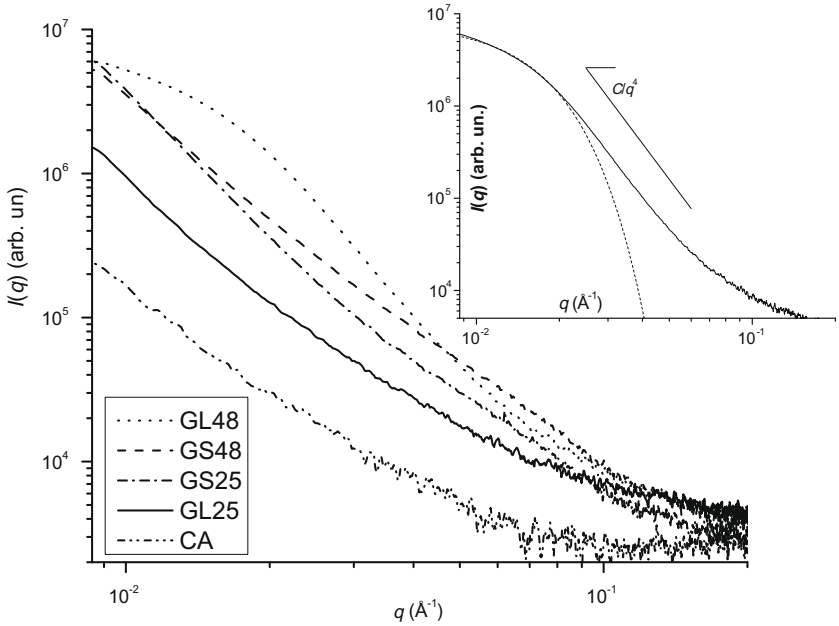

Fig. 12. Synchrotron small angle X-ray scattering (SAXS) of cellulose acetate (CA) and cellulose acetate-*g*-poly(MDEGMA) copolymers with long (GL) or short (GS) grafts. Insert: GL44 data (solid line) and modelling with Guinier's law (dashed line) and Porod's asymptote.

showing that the diffraction pattern of cellulose acetate varies with the value of DS_{Ac}. In this work, the obtained WAXS pattern was characteristic of an amorphous or very weakly crystalline cellulose acetate.

At small angles, the scattered intensity decreased as a function of the scattering vector q over a range of several decades from 8×10^{-3} Å^{-1} to 0.2 Å^{-1} as shown in Fig. 12. Cellulose acetate displayed a weak but complex scattering diagram that could not be analyzed through standard procedures used to deduce characteristic sizes. Meanwhile, it can be deduced from the obtained results that the electron density fluctuations inducing SAXS in cellulose acetate films are large (i.e. with characteristic size larger than 50 nm). The complexity of the structural organization of cellulose acetate solutions in butanone or acetone is well recognized through several studies of intermolecular aggregation [25–27]. Light scattering measurements and size exclusion chromatography [27] evidenced microgels rich in cellulose triacetate blocks (partly crystalline microregions). Such heterogeneities are likely to develop as concentration increases with film formation and subsist in the final morphology of the films in solid state [26].

Graft copolymers exhibited higher scattered intensities than cellulose acetate by a factor 10 and above, the stronger scatterers (GS48 and GL44) being the grafted copolymers with the highest weight fractions of poly(MDEGMA). GS48, GS25 and GL25 samples showed scattered patterns qualitatively comparable to that of cellulose acetate. This reflects the effect of grafting on the contrast factor of large scale heterogeneities. If cellulose triacetate (CTA) blocks contribute to form such heterogeneities [27], then the grafted poly(MDEGMA) should be preferentially located in the regions that initially contained more cellulose diacetate (CDA) residues. Grafting is thus likely to increase the electron density difference between CTA-rich and poly (MDEGMA)-rich zones. For the copolymer with 44 wt.% of long grafts (GL44), the log–log plot of scattered intensity vs. q exhibited the usual q^{-4} relation above $q \sim 2.5 \times 10^{-2}$ Å^{-1} and thus followed a Porod's law characteristic for a two-phase material with sharp interface. In the smaller q-range, the Guinier's law was applied to estimate the size of nano-domains according to Eq. (7):

$$I(q) = NV_p^2 \times (\Delta\rho)^2 \times \exp\left(-\frac{R_g^2}{3}q^2\right) \quad (7)$$

where N is the number of nano-domains in the sample volume, V_p is the nano-domain volume and $\Delta\rho$ is difference between the electron density within the nano-domains and in the outer matrix, R_g is the mean radius of gyration the nano-domains. The value of R_g deduced from the slope of the Guinier plot (i.e. $\log_e(I(q))$ vs. q^2,) was close to 11.5 nm (see insert in Fig. 12).

The morphology of GL44 can thus be described as being heterogeneous at different length scales. At larger characteristic distances, micron-size domains rich in CTA residues and therefore poorer in grafted segments should be present, like in all graft copolymers, as a result of the heterogeneous distribution of acetate groups in cellulose acetate. At a smaller scale, nano-domains possibly resulting from segregated poly(MDEGMA) grafts induce some additional heterogeneity most likely in the amorphous matrix surrounding the CTA-rich microdomains.

4. Conclusion

Two series of cellulose acetate-*g*-poly(MDEGMA) copolymers were obtained by ATRP on the basis of a

"grafting from" method. A first macroinitiator led to a series of cellulose acetate-*g*-poly(MDEGMA) copolymers with a high number of short grafts. The graft polydispersity was at best close to 1.5. A second macroinitiator led to a second series of graft copolymers with a small number of long grafts. In this case, the ATRP control was limited to the very low conversion range (0–15%) in good agreement with the rare results reported so far for the ATRP grafting of cellulose acetate with other monomers [22,28,29]. The successful synthesis scaling-up up to ca. 5 g of copolymer samples eventually led to two series of cellulose acetate-*g*-poly(MDEGMA) copolymers with almost the same graft weight fractions but different architectures.

Their morphology – which is believed to play a key role in their permeability properties – was then characterized by synchrotron X-ray scattering. The poly(MDEGMA) grafts appeared much less segregated for the copolymers with short grafts. On the contrary, the copolymers with the long grafts displayed a phase segregation which increased with the copolymer graft content. The copolymer with 44 wt.% of long grafts eventually showed a fully segregated morphology with sharp interfaces and a radius of gyration of 11.5 nm was estimated for the corresponding nano-domains.

Last but not least, the new graft copolymers are very good film-forming materials which appear really promising for the separation of alcohol/ether mixtures by pervaporation. We have reported very recently their membrane properties for the purification of ethyl-*tert*-butyl ether (ETBE), one of the leading bio-fuels in the European Union. A comparison with the related literature results has shown that the graft copolymers investigated in this work are amongst the best membrane materials so far reported for the purification of ETBE by the pervaporation membrane separation process [30].

Acknowledgments

CNRS (le Centre National de la Recherche Scientifique) and ADEME (l'Agence de l'Environnement et de la Maîtrise de l'Energie) are gratefully acknowledged for their financial support.

References

[1] Edgar KJ, Buchanan CM, Debenham JS, Rundquist PA, Seiler BD, Shelton MC, et al. Prog Polym Sci 2001;26:1605–88.
[2] Uragami T. Structures and functionalities of membranes from polysaccharide derivatives. In: Dumitriu S, editor. Polysaccharides. New York: Marcel Dekker, Inc.; 2005. p. 1087–122.
[3] Wang J-S, Matyjaszewski K. J Am Chem Soc 1995;117:5614–5.
[4] Kato M, Kamigaito M, Sawamoto M, Higashimura T. Macromolecules 1995;28:1721–3.
[5] Matyjaszewski K, Spanswick J. Mater Today 2005;8:26–33.
[6] Carlmark A, Malmström E. J Am Chem Soc 2002;124:900–1.
[7] Lindqvist J, Malmström E. J Appl Polym Sci 2006;100:4155–62.
[8] Coskun M, Temuez MM. Polym Int 2005;54:342–7.
[9] Lee SB, Koepsel RR, Morley SW, Matyjaszewski K, Sun Y, Russell AJ. Biomacromolecules 2004;5:877–82.
[10] Singh N, Chen Z, Tomer N, Wickramasinghe SR, Soice N, Husson SM. J Membr Sci 2008;311:225–34.
[11] Westlund R, Carlmark A, Hult A, Malmstroem E, Saez IM. Soft Matter 2007;3:866–71.
[12] Plackett D, Jankova K, Egsgaard H, Hvilsted S. Biomacromolecules 2005;6:2474–84.
[13] Zhou Q, Greffe L, Baumann MJ, Malmstroem E, Teeri TT, Brumer III H. Macromolecules 2005;38:3547–9.
[14] Sui X, Yuan J, Zhou M, Zhang J, Yang H, Yuan W, et al. Biomacromolecules 2008;9:2615–20.
[15] Ifuku S, Kadla JF. Biomacromolecules 2008;9:3308–13.
[16] Lutz J-F, Hoth A. Macromolecules 2006;39:893–6.
[17] Yamamoto S, Pietrasik J, Matyjaszewski K. Macromolecules 2007;40:9348–53.
[18] Matyjaszewski K, Shipp DA, Wang J-L, Grimaud T, Patten TE. Macromolecules 1998;31:6836–40.
[19] Hansen NML, Haddleton DM, Hvilsted S. J Polym Sci, Part A: Polym Chem 2007;45:5770–80.
[20] Fischer H. J Polym Sci, Part A: Polym Chem 1999;37:1885–901.
[21] Tezuka Y, Tsuchiya Y. Carbohydr Res 1995;273:83–91.
[22] Vlcek P, Janata M, Latalova P, Dybal J, Spirkova M, Toman L. J Polym Sci, Part A: Polym Chem 2007;46:564–73.
[23] Guinier A. X-ray diffraction in crystals, imperfect crystals, and amorphous bodies: Courier Dover Publications; 1994 (ISBN 0486680118).
[24] Barud HS, de Araujo Junior AM, Santos DB, de Assunçao RMN, Meireles CS, Cerqueira DA, et al. Thermochim Acta 2008;471:61–9.
[25] Suzuki H, Muraoka Y, Satio M, Kamide K. Eur Polymer J 1982;18:831–7.
[26] Goebel KD, Berry GC, Tanner DW. J Polym Sci Polym Phys Ed 1979;17:917–37.
[27] Fleury E, Dubois J, Léonard C, Joseleau JP, Chanzy H. Cellulose 1994;1:131–44.
[28] Shen D, Huang Y. Polymer 2004;45:7091–7.
[29] Vlcek P, Janata M, Latalova P, Kriz J, Cadova E, Toman L. Polymer 2006;47:2587–95.
[30] Billy M, Ranzani Da Costa A, Lochon P, Clement R, Dresch M, Jonquieres A. J Membr Sci 2010;348:389–96.
[31] Shen D, Yu H, Huang Y. J Polym Sci, Part A: Polym Chem 2005;43:4099–108.
[32] Kang H, Liu W, He B, Shen D, Ma L, Huang Y. Polymer 2006;47:7927–34.
[33] Tang X, Gao L, Fan X, Zhou Q. J Polym Sci, Part A: Polym Chem 2007;45:1653–60.
[34] Shen D, Yu H, Huang Y. Cellulose 2006;13:235–44.
[35] Östmark E, Harrisson S, Wooley KL, Malmström EE. Biomacromolecules 2007;8:1138–48.
[36] Kang H, Liu W, Liu R, Huang Y. Macromol Chem Phys 2008;209:424–30.
[37] Östmark E, Nyström D, Malmström E. Macromolecules 2008;41:4405–15.
[38] Li Y, Lui R, Liu W, Kang H, Wu M, Huang Y. J Polym Sci, Part A: Polym Chem 2008;46:6907–15.